Theoretical comparison between field emission from single-wall and multi-wall carbon nanotubes

A. Mayer,[1,*] N. M. Miskovsky,[2] and P. H. Cutler[2]
[1]*Laboratoire de Physique du Solide, Facultés Universitaire N.-D. de la Paix, Rue de Bruxelles 61, B-5000 Namur, Belgium*
[2]*Departments of Physics, 104 Davey Lab, Penn State University, University Park, Pennsylvania 16802*
(Received 21 November 2001; published 4 April 2002)

We present three-dimensional simulations of field emission from single-wall and multi-wall carbon nanotubes. The structures considered are the metallic ideally open (5,5), (10,10), (15,15) and (5,5)@(10,10)@(15,15) nanotubes. For the multi-wall structure, flat and convex terminations are considered. The scattering calculations are achieved using a transfer-matrix methodology and band-structure effects result from using pseudopotentials and repeating periodically a basic unit of the nanotubes. The electronic emission from the single-wall nanotubes considered is found to decrease linearly with the radius of the tube. Multi-wall nanotubes are better emitters than single walls, the current extracted from multi-wall structures being higher than the total current obtained by considering their single-wall layers separately. The current emitted from a multi-wall structure is still increased when the termination is convex (instead of flat). The reduced polarizability of multi-wall nanotubes (compared to single-wall structures) is an important aspect for explaining their field-emission properties.

DOI: 10.1103/PhysRevB.65.155420 PACS number(s): 73.63.Fg, 79.70.+q, 85.35.Kt, 03.65.Nk

I. INTRODUCTION

Carbon nanotubes show interesting field-emission properties such as low extraction field, high current density, and long operating time. In general, the current-voltage characteristics of carbon nanotubes are found to follow a Fowler-Nordheim type tunneling law[1–4] with an emitter work function around 5 eV depending on the type of nanotube. Electronic states localized near or at the apex of the nanotube influence the current emission profile.[5,6] These localized states are relatively well documented for various kinds of tube termination[7–10] and can be induced by the extraction field.[11] It is assumed in most calculations that the dangling bonds are not saturated although it is recognized that in ambient conditions hydrogen may saturate them.[12]

In extension of previous simulations of field emission from carbon nanotubes,[13–16] we now consider the dependence of the emission from single-wall nanotubes on the radius of the tube and compare these results with those obtained with multi-wall structures. The methodology used in this paper is the transfer-matrix technique developed in previous publications.[17–19] The potential energy is calculated using the pseudopotentials of Bachelet *et al.*[20] In addition, in order to reproduce band-structure effects, a basic unit of the nanotubes is repeated periodically in an intermediate region between the supporting metallic substrate and that containing the fields (see Fig. 1).

The main features of this model are described in Sec. II. Section III presents results of field emission from single-wall and multi-wall nanotubes, for a given local electric field of 2.5 V/nm. The current emitted from single-wall structures is found to decrease linearly with the radius of the tube. Multi-wall nanotubes are better emitters than single-wall structures, the current extracted from multi-wall nanotubes being higher than that obtained by considering their single-wall layers individually. Using multi-wall nanotubes with a convex termination (instead of a flat one) further improves the emission.

II. THEORY

The geometry considered in this paper is depicted in Fig. 1. The nanotube is located between a metallic substrate (region I, $z \leqslant -N \times a$) and the field-free vacuum (region III, $z > D$). The intermediate region consists of a field-free region $-a \times N \leqslant z \leqslant 0$, which contains N periodic repetitions of a basic unit of the nanotube, and region II ($0 \leqslant z \leqslant D$), which contains the part of the nanotube subject to the extraction field. This field results from an electric bias V, which is established between the two limits of region II. The field-free intermediate region $-N \times a \leqslant z \leqslant 0$ is an artificial part of the model, which is introduced for the purpose of reproducing appropriate band-structure effects (intrinsic to the nanotube) in the distribution of incident states and is not related to an experimental picture, where nonzero fields would remain until the metallic support in region I. Due to the nanometric dimensions of both the nanotube and the cathode-anode distance D used in our simulations, the applied electric field V/D (2.5 V/nm) should be regarded as a *local* field, i.e., as already magnified by a micron-long nanotube body, in order to account for experimental fields being typically of a few volts per micron.

The potential energy in region II is calculated by using techniques of Ref. 18, with a pseudopotential for the ion-core potential.[20] The electronic density associated with the four valence electrons of each carbon atom are represented by the sum of two Gaussian distributions (with parameters given in Ref. 20). These electronic densities are displaced from the nuclear positions according to the polarization $\mathbf{p}_j$ of the corresponding carbon atom. The dipoles $\mathbf{p}_j$ are calculated[17] by taking account of the extraction field, dipole-dipole interactions, and the anisotropic polarizability[21] of the carbon atoms. The electronic exchange energy is evaluated by using the local density approximation $\frac{4}{3} C_X \rho^{1/3}$, where $\rho(\mathbf{r})$ is the local electronic density[18] and $C_X = -3/4(e^2/4\pi\epsilon_0)(3/\pi)^{1/3}$.

To compute electron scattering from the metallic substrate (region I) to the vacuum (region III), we used the transfer-

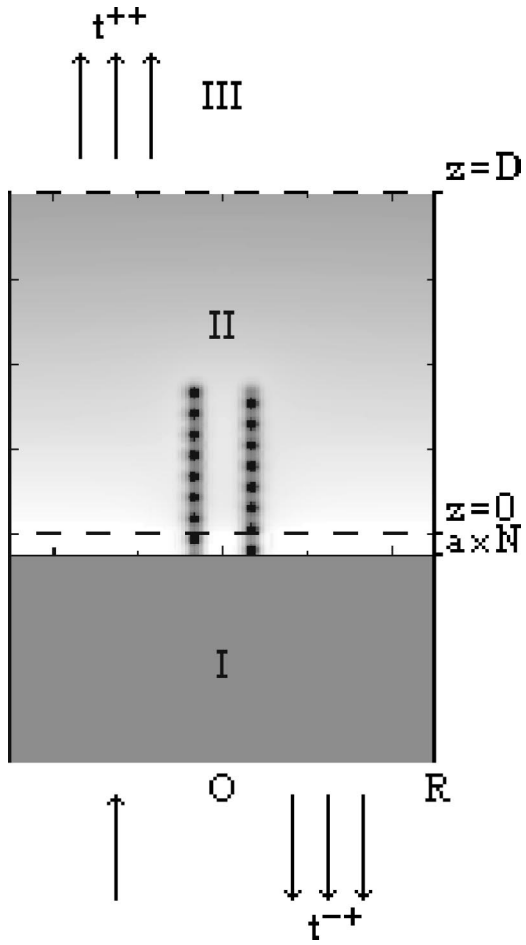

FIG. 1. Schematic depicting of the geometry of the nanotube field emission process. Region I ($z \leqslant -a.N$) is a perfect metal. The intermediate region $-a.N \leqslant z \leqslant 0$ contains N periodic repetitions of a basic unit of the (10,0) nanotube. Region II ($0 \leqslant z \leqslant D$) contains the part of the nanotube subject to the electric field. Region III ($z > D$) is the field-free vacuum. The arrows in the regions I and III symbolize scattering solutions, with a single incident state in region I and the corresponding reflected and transmitted states (whose coefficients are contained in the transfer matrices t^{-+} and t^{++} respectively).

matrix technique described in Refs. 17–19. In this formulation, the electrons involved in the transport remain localized inside a cylinder of radius R in the regions preceding the vacuum region III (R is chosen large enough so the results are independent of its particular value). Making use of the cylindrical symmetry in the problem, the wave function is expanded in terms of basis states in region I as $\Psi^{I,\pm}_{m,j} = A_{m,j} J_m(k_{m,j}\rho)\exp(im\phi)\exp[\pm i\sqrt{(2m/\hbar^2)(E-V_{\text{met}})}z]$ and in the anode plane $z=D$ as $\Psi^{D,\pm}_{m,j} = A_{m,j} J_m(k_{m,j}\rho)\exp(im\phi)\exp[\pm i\sqrt{(2m/\hbar^2)E}z]$, where the $A_{m,j}$ are normalization coefficients, J_m Bessel functions, $k_{m,j}$ transverse wave vectors solutions of $J_m(k_{m,j}R)=0$, E the electron energy, and V_{met} is the potential energy in the supporting metal. The $\pm$ signs refer to the propagation direction relative to the z axis, which is oriented from region I to region III. The transfer-matrix methodology[17] then provides scattering solutions of the form

$$\Psi^{+}_{m,j} \overset{z\leqslant -a\times N}{=} \Psi^{I,+}_{m,j} + \sum_{m',j'} t^{-+}_{(m',j',m,j)} \Psi^{I,-}_{m',j'} \overset{z\geqslant D}{=} \sum_{m',j'} t^{++}_{(m',j'),(m,j)} \Psi^{D,+}_{m',j'}, \quad (1)$$

corresponding to single incident states $\Psi^{I,+}_{m,j}$ with a unit amplitude (the t^{-+} and t^{++} matrices are defined in Fig. 1). Total current densities result from the contribution of every solution associated with a propagative incident state in the supporting metal.

III. APPLICATION: FIELD EMISSION FROM SINGLE-WALL AND MULTI-WALL NANOTUBES

We previously investigated field emission from single-wall semiconducting (10,0) and metallic (5,5) carbon nanotubes.[13–16] For these structures, the total-energy distribution of field-emitted electrons exhibits the gap of the (10,0) nanotube[15,22] as well as peaks, which are related to both the van Hove singularities[23] in the distribution of states, and stationary waves in the carbon nanotube structure.[14,15] As expected, metallic nanotubes are found to be better emitters than semiconducting ones. Due to field penetration being more pronounced in open structures than in closed ones, single-wall open structures are predictably better emitters than closed ones. The current enhancement following hydrogen saturation of the dangling bonds of the open (5,5) structure was presented in Ref. 13. Finally, we investigated in Ref. 16 the efficiency of a photostimulation to increase the emission. It turns out that photostimulation can increase, by orders of magnitude depending on the photon energy and the power-flux density of the radiation, the current emitted from the semiconducting (10,0) structure, thus providing an efficient way to control the rate of emission (by the radiation instead of the electric field). In this paper, we study the dependence of the emission on the tube radius (for single-wall nanotubes) and compare these results with those obtained with multi-wall structures.

Since our objective is to achieve high rates of emission, only metallic nanotubes will be considered, i.e., the single-wall (5,5), (10,10), and (15,15) nanotubes and the multi-wall (5,5)@(10,10)@(15,15) combining these three first structures (see Ref. 24 for energy considerations). The nanotubes are ideally open (i.e., without hydrogen saturation). They all have $N=16$ periodic repetitions of their basic unit in the field-free region between the metallic substrate $z \leqslant -Na$ and the region $0 \leqslant z \leqslant D$ where the fields are present. For the purpose of reflecting the properties of infinite nanotubes, the metal in region I is given an internal potential energy 16 eV lower than the vacuum level and a Fermi level adjusted to the middle of the metallic plateau in the energy distribution of incident states (which is 5.25 eV below the vacuum level). The region $0 \leqslant z \leqslant D$ containing the fields always includes seven basic units of the nanotubes, except for the case where a convex termination is considered for the multi-wall structure (this case is described below). The basic units of the (5,5), (10,10), and (15,15) nanotubes all have the

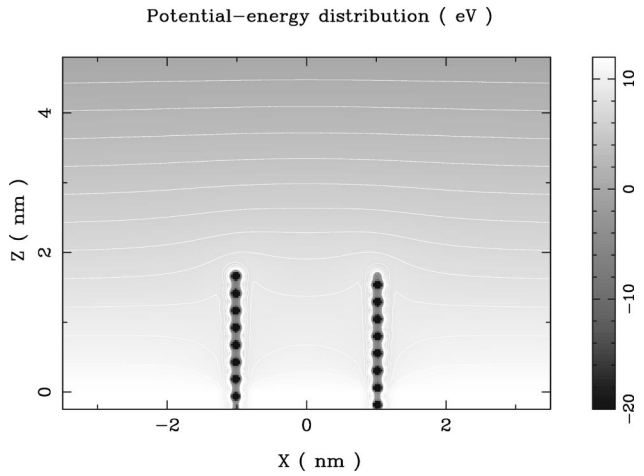

FIG. 2. Potential-energy distribution (section in the *xz* plane) corresponding to an open (15,15) nanotube, a cathode-anode distance of 4.8 nm and a bias of 12 V.

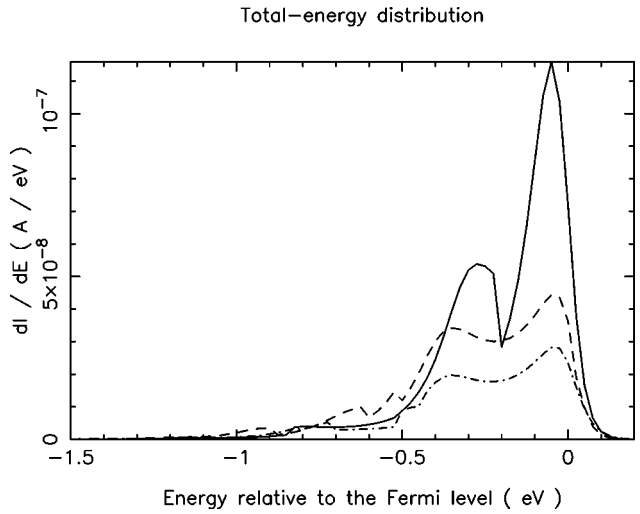

FIG. 3. Total-energy distribution of electrons field emitted, respectively, from single-wall (5,5) (solid), (10,10) (dashed), and (15,15) (dot-dashed) nanotubes, for an extraction field of 2.5 V/nm.

same length a of 0.246 nm and radii, respectively, of 0.339, 0.678, and 1.017 nm. The multi-wall (5,5)@(10,10)@(15,15) nanotube (with flat termination) is the combination of these three structures. See Fig. 1 for a schematic depiction.

The simulations all assume the same extraction field V/D of 2.5 V/nm (the bias V is 12 V and the cathode-anode distance D is 4.8 nm). This local field value results from the geometric enhancement of the applied macroscopic field on the micron long emitter. Finally the temperature T is taken to be 298 K.

A. Field-emission from (5,5), (10,10), and (15,15) single-wall nanotubes

Let us consider the single-wall (5,5), (10,10), and (15,15) nanotubes of equal length. They are metallic and have similar band structures. They have the same length. The radius of the (10,10) and (15,15) structures is, respectively, two and three times that of the (5,5) structure. Differences in the field-emission properties are therefore essentially due to geometrical factors and to the shape of the potential barrier facing the emitter.

The potential-energy distribution associated with the (15,15) structure is illustrated in Fig. 2 [the distribution corresponding to the (5,5) structure appears, with less details, in Fig. 1]. The lines in the figure indicate equipotentials associated with integer values (1,2, . . . ,11 eV). The total-energy distributions of the electrons that are emitted from the (5,5), (10,10), and (15,15) structures are illustrated in Fig. 3.

The distributions are similar and exhibit peaks at the same position. As explained in Ref. 14, these peaks are related to stationary waves in the structure (their number increases with the length of the nanotube). The fact they appear at the same position is due to the fact the three structures have the same length (and the same internal potential energy). Experimental observation of peaks in the total-energy distributions of carbon nanotubes is reported in Refs. 3,6.

The currents extracted from the (5,5), (10,10), and (15,15) nanotubes are, respectively, 0.298×10^{-7}, 0.205×10^{-7}, and 0.124×10^{-7} A. Considering the radii are 1, 2, and 3 times 0.339 nm, we see that the current extracted from these carbon nanotubes decreases with the radius and that this decrease is essentially linear. This reduction of the current is a consequence of the field amplification factor β decreasing with the tube radius (due to a diminishing aspect ratio), as demonstrated by Adessi *et al.*[25]

B. Field emission from (5,5)@(10,10)@(15,15) multi-wall nanotubes

The first multi-wall nanotube considered is the (5,5)@(10,10)@(15,15), structure consisting of the three previous single-wall structures. It has the same length and radius as the single-wall (15,15) nanotube and the termination is flat.

The potential-energy distribution associated with this structure is illustrated in Fig. 4. Although the length is the same as in the previous case, the equipotential facing the multi-wall nanotube is at 7 eV, while it was at 8 eV for the three previous single-wall structures. This observation means that for the same length, the potential barrier facing a multi-wall nanotube is lower than that facing a single wall, so the electronic emission is larger as explained below.

The reason for the potential barrier being lower comes partly from the dipole-dipole interactions between neighboring tubes, which reduces the response of the system to the external field. The polarization of the nanotube is therefore smaller and the field penetration higher. This explains why the facing equipotential is smaller than in situations where the tendency of equipotentials to bypass the emitter is more pronounced because of a higher polarization of the structure.

The total-energy distribution corresponding to the flat multi-walled nanotube is shown in Fig. 5. The distribution is dominated by peaks, which are sharper than for the single walled nanotubes shown in Fig. 3. We also note the appearance of additional peaks in Fig. 5. A reason for both the increased number and sharpness is the size effect, that is, the

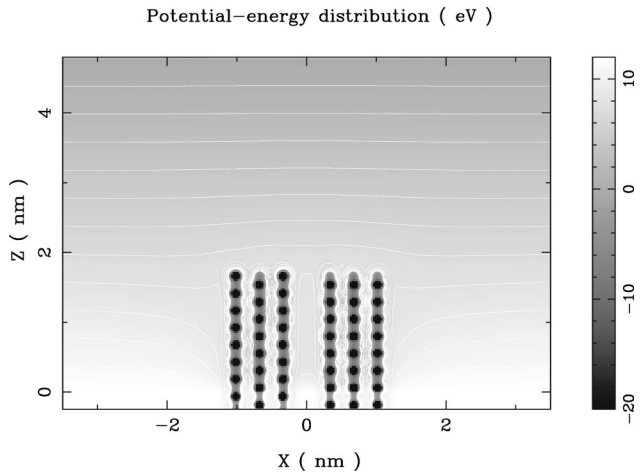

FIG. 4. Potential-energy distribution (section in the *xz* plane) corresponding to an open (5,5)@(10,10)@(15,15) nanotube with flat termination, a cathode-anode distance of 4.8 nm and a bias of 12 V.

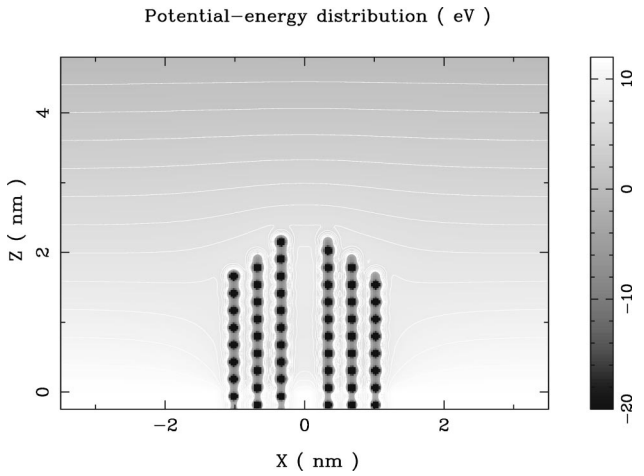

FIG. 6. Potential-energy distribution (section in the *xz* plane) corresponding to an open (5,5)@(10,10)@(15,15) nanotube with convex termination, a cathode-anode distance of 4.8 nm and a bias of 12 V.

larger diameter of multi-walled nanotubes can accommodate additional propagating states which are channeled into a narrower discrete energy range due to the strong interaction between the walls of the composite nanotube. An analog for this phenomenon would be propagation of electromagnetic waves in a coaxial waveguide. We noticed that the potential wells on the carbon atoms are deeper for the multi-wall nanotube than for the single-wall structures (the energy distributions represented in Figs. 2, 4, and 6 are truncated). These deeper potentials are due to the displacement of the electronic charges of the carbon atoms being larger (because of increased interactions between the atoms in the different layers), so that the screening of the nuclear charge is less efficient. These deeper atomic potentials also contribute to sharper peaks.

The total current extracted from this multi-wall structure is 0.869×10^{-6} A. This value is 14 times the sum of the currents extracted from the (5,5), (10,10), and (15,15) structures separately. The reason for that is, of course, that the facing potential barrier is lower.

The next multi-wall structure considered has a convex termination. The central (5,5) structure has nine basic units in region II, the intermediate (10,10) eight units, and the external (15,15) seven units as in the previous case. The corresponding potential-energy distribution is illustrated in Fig. 6. The equipotential facing the emitter is approximately at 7 eV, but the extreme apex of the physical structure extends slightly above that equipotential surface. Thus, the emission is expected to be enhanced (the situation is close to breakdown, where electrons would travel ballistically over the potential barrier).

The total-energy distribution of the electrons emitted from this structure is illustrated in Fig. 7. The distribution is dominated by a peak, which is related to the central, longest part

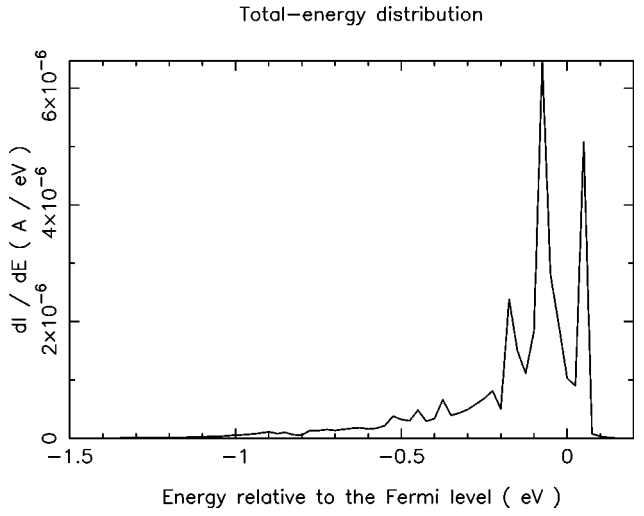

FIG. 5. Total-energy distribution of electrons field-emitted from a multi-wall (5,5)@(10,10)@(15,15) nanotube with flat termination, for an extraction field of 2.5 V/nm.

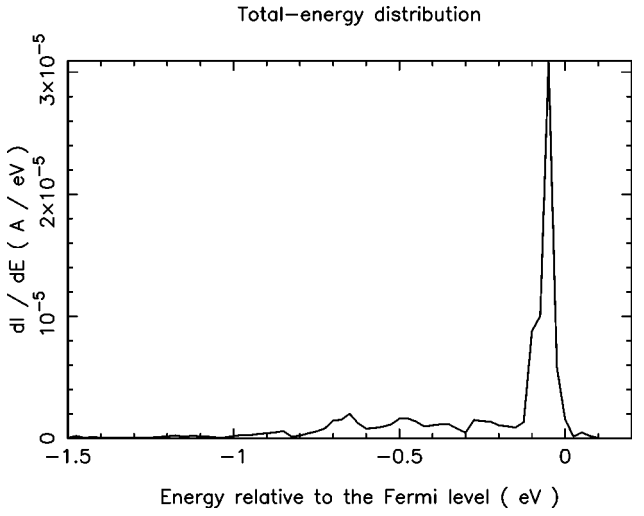

FIG. 7. Total-energy distribution of electrons field-emitted from a multi-wall (5,5)@(10,10)@(15,15) nanotube with convex termination, for an extraction field of 2.5 V/nm.

of the nanotube. The current extracted in this case is 0.214×10^{-5} A. This value is 2.5 larger than for the flat structure, which is expected from our previous comments on the potential energy.

We conclude that multi-wall nanotubes with a convex termination are better emitters than with a flat one. It has to be noted that closed single-wall nanotubes were observed[5,13,14] to be less efficient emitters than open ones. Single-wall nanotubes have a stronger tendency to polarize in response to the field. When these structures are closed, the screening of the electric field is increased, the lowering of the potential barrier less pronounced and therefore the current reduced. The response of multi-wall structures to the external field is, however, less pronounced, so their extension to achieve a convex termination essentially results in a deeper penetration into the potential barrier, which here increases the emission. This difference between single-wall and multi-wall nanotubes in the response to the electric field explains these opposing effects on the emission. This comment, however, needs to be tempered by the fact that open multi-wall nanotubes with convex termination are not closed multi-wall structures. Our observations are, however, supported by the measurements of Bonard *et al.*,[2] according to whom closed multi-wall nanotubes (so extended structures such as those discussed here) are better emitters than open ones.

Finally we compare these last results with those corresponding to a single-wall (5,5) nanotube having nine basic units in region II, i.e., the internal tube of the convex-terminated (5,5)@(10,10)@(15,15). The current obtained for this elongated (5,5) nanotube is 0.358×10^{-6} A. This is 6 times less than the current extracted from the convex-terminated (5,5)@(10,10)@(15,15) [and even 2.4 less than the current extracted from the flat-terminated (5,5)@(10,10)@(15,15), which is shorter]. The significance of this comparison is that the emission from the convex-terminated (5,5)@(10,10)@(15,15) multi-walled nanotube is not only due to its inner, longer tube but there is a collective effect due to three tubes contributing to the emission. This collective effect reduces the response of the whole nanotube to the external field and thus lowers the facing potential barrier.

IV. CONCLUSION

In this paper, we have investigated field emission from ideal (i.e., unrelaxed and unsaturated) single-wall and multi-wall carbon nanotubes. Comparisons between single-wall nanotubes of different radii and the corresponding multi-wall structures (with flat or convex termination) were considered.

The technique used for these simulations takes account of the three-dimensional aspects of the problem (i.e., the atomic configuration and the potential barrier associated with field emission). The local field was estimated to be a few V/nm based on a geometric enhancement of the experimentally applied macroscopic field of a few V/micron.

The current extracted from single-wall nanotubes was observed to decrease with the radius of the structure. This observation agrees with calculations of Adessi *et al.*,[25] where the field amplification factor β of nanotubes is also found to decrease with the radius. For larger radii, the increase of the emitting area may have more influence on the emission than the decrease of the β factor, so in this case the current could increase with the radius. This regime, however, for numerical reasons, is out of reach of this technique so our conclusions only apply to diameters of a few nanometers.

Multi-wall nanotubes were observed to be better emitters than single-wall nanotubes. This conclusion is in agreement with measurements of Bonard *et al.*[2] The main reason found in this paper is the smaller polarization of the structure, which is responsible for the facing potential barrier being lower. This lower global polarizability of multi-wall nanotubes means that an essential aspect of any protrusion of these structures is a deeper penetration of the emitter apex in the potential barrier (resulting in an enhanced emission). Indeed multi-wall nanotubes were shown to be better emitters when the termination is convex (instead of flat) and it is usually observed[2] that closed multi-wall nanotubes are better emitters than open ones (despite the fact that the screening of the electric field should be more efficient for closed structures). It is to be noted that the screening of the electric field is the dominating aspect when closing single-wall nanotubes, as closed (5,5) single-wall nanotubes were demonstrated[13,14] to emit less current than the corresponding open structures. This last observation implies that a compromise between higher penetration in the potential barrier and better screening of the electric field probably exists for closed multi-wall nanotubes, explaining why they are not always observed to emit more current than open ones.

ACKNOWLEDGMENTS

This work was supported by the National Fund for Scientific Research (FNRS) of Belgium and by NSF Grant No. DMI-0078637 administrated by UHV Technologies, Inc., Mt. Laurel, NJ. One of the authors (A.M.) acknowledges the use of the Namur Scientific Computing Facility. The authors also thank Ph. Lambin for useful discussions.

*Corresponding author. Electronic address: alexandre.mayer@fundp.ac.be

[1] W.A. de Heer, A. Chatelain, and D. Ugarte, Science **270**, 1179 (1995).

[2] J.M. Bonard, J.P. Salvetat, T. Stöckli, L. Forró, and A. Chatelain, Appl. Phys. A: Mater. Sci. Process. **69**, 245 (1999) , and references therein.

[3] M.J. Fransen, Th.L. van Rooy, and P. Kruit, Appl. Surf. Sci. **146**, 312 (1999) , and references therein.

[4] P.G. Collins and A. Zettl, Phys. Rev. B **55**, 9391 (1997).

[5] Ch. Adessi and M. Devel, Phys. Rev. B **62**, 13 314 (2000).

[6] K.A. Dean, O. Groening, O.M. Kuttel, and L. Schlapbach, Appl. Phys. Lett. **75**, 2773 (1999).

[7] R. Tamura and M. Tsukada, Phys. Rev. B **52**, 6015 (1995).

[8] D.L. Carroll, P. Redlich, P.M. Ajayan, J.C. Charlier, X. Blase, A. De Vita, and R. Car, Phys. Rev. Lett. **78**, 2811 (1997).

[9] A. De Vita, J.Ch. Charlier, X. Blase, and R. Car, Appl. Phys. A: Mater. Sci. Process. **68**, 283 (1999).
[10] Ph. Kim, T.W. Odom, J.L. Huang, and C.M. Lieber, Phys. Rev. Lett. **82**, 1225 (1999).
[11] S. Han and J. Ihm, Phys. Rev. B **61**, 9986 (2000).
[12] M.S.C. Mazzoni, H. Chacham, P. Ordejon, D. Sanchez-Portal, J.M. Soler, and E. Artacho, Phys. Rev. B **60**, 2208 (1999).
[13] A. Mayer, N.M. Miskovsky, and P.H. Cutler, Appl. Phys. Lett. **79**, 3338 (2001).
[14] A. Mayer, N.M. Miskovsky, and P.H. Cutler, Ultramicroscopy (to be published).
[15] A. Mayer, N.M. Miskovsky, and P.H. Cutler, J. Vac. Sci. Technol. **20**, 100 (2002).
[16] A. Mayer, N. M. Miskovsky, and P. H. Cutler, Phys. Rev. B (to be published).
[17] A. Mayer and J.-P. Vigneron, Phys. Rev. B **56**, 12 599 (1997).
[18] A. Mayer, P. Senet, and J.-P. Vigneron, J. Phys.: Condens. Matter **11**, 8617 (1999).
[19] A. Mayer and J.-P. Vigneron, J. Phys.: Condens. Matter **10**, 869 (1998); Phys. Rev. B **60**, 2875 (1999); Phys. Rev. E **59**, 4659 (1999) ; **61**, 5953 (2000).
[20] G.B. Bachelet, H.S. Greenside, G.A. Baraff, and M. Schluter, Phys. Rev. B **24**, 4745 (1981).
[21] P.A. Gravil, Ph. Lambin, G. Gensterblum, L. Henrard, P. Senet, and A.A. Lucas, Surf. Sci. **329**, 199 (1995).
[22] M. S. Dresselhaus, G. Dresselhaus, P. C. Eklund, and R. Saito, in *Optical and Electronic Properties of Fullerenes and Fullerene-Based Materials*, edited by J. S. Shinar, Z. V. Vardeny, and Z. H. Kafafi (Dekker, New York, 2000), p. 236.
[23] J. M. Ziman, *Principles of the Theory of Solids* (Cambridge University Press, Cambridge, 1964), p. 46.
[24] Y.-K. Kwon and D. Tománek, Phys. Rev. B **58**, 16 001 (1998).
[25] Ch. Adessi and M. Devel, J. Vac. Sci. Technol. B (to be published).